

Spectroscopic studies, phonon dispersion and heat capacity of poly (vinylidene chloride)

Eram Anis¹, Parvej Ali², Seema Srivastava¹, M.W. Baig³ and Moiz Ahmad¹

¹ Department of Physics, Integral University, Lucknow-226026, U.P., India

² Department of Chemistry, Integral University Campus, Shahajahanpur-242306, India

³ Department of Mechanical Engineering, Integral University Campus, Shahajahanpur-242306, U.P., India

Received April 2015; Accepted July 2015

ABSTRACT

Poly (vinylidene chloride) (PVDC) is a barrier polymer which has a wide scope in food packaging industries. A comprehensive study of the normal modes and their dispersion in PVDC using Wilson's GF matrix method as modified by Higgs is reported. It provides a detailed interpretation of IR and Raman spectra. Characteristic feature of dispersion curves, such as regions of high density-of-states, repulsion, and character mixing of dispersion modes, are discussed. Heat capacity has been calculated in the range 50–500 K via density-of-states using Debye relation. It is in fairly good agreement with the experimental data. Heat capacity behavior of PVDC with temperature was observed nearly linear in nature. Heat capacity provides a relationship between microscopic behavior and a macroscopic property. The thermal stability of a polymeric system and its interactive nature with other properties, such as phonon-phonon coupling is also related to thermodynamic behavior. The present study provides a theoretical framework to understand experimental measurements.

Keywords: Poly (vinylidene chloride); Vibrational dynamics; IR; Raman Spectroscopy; Heat Capacity

INTRODUCTION

Barrier polymers, such as polyethylene (PE), polypropylene (PP), polyvinyl alcohol (PVOH) and poly (vinylidene chloride) (PVDC), have played a key role in this evolution towards alternative packaging materials while preserving the long term stability and quality of the wrapped product. However, polyethylene and polypropylene only display a high impermeability to water, PVOH only to oxygen while PVDC offers a more complete protection, owing to its excellent

barrier properties towards water, oxygen and aroma, as well as chemical resistance to a large variety of solvents [1-5].

Vinylidene chloride (VDC) polymerizes via both free-radical and ionic reactions. Anionic polymerization of VDC may be carried out [6]. However the use of anionic catalysts is often undesirable as it leads to extensive degradation of the polymer [7]. For instance the polymerization of vinylidene chloride catalyzed by butyl lithium has been reported, but resulting

*Corresponding author: aliparvez85@gmail.com

polymers exhibited low molecular weights and low chlorine contents, due to side reactions involving the elimination of chlorine atoms as lithium chloride from the polymer chains. Due to the strong electron withdrawing effect of chlorine atoms, vinylidene chloride is not susceptible to be polymerized via cationic catalysis [6].

Radical processes are thus by far the most employed. Free-radical polymerization of VDC has been studied in solution, in a solvent that dissolves both the monomer and the polymer [8]. Polymerizations of VDC in bulk or in solvents, such as hexane or benzene, have also been reported at the laboratory scale and enabled to gain a better understanding of polymerization kinetics [9].

Vibrational spectroscopy plays a very important role in elucidating polymer structure and normal mode analysis. It provides a better identification of various vibrational modes and interpretation of IR and Raman spectra. Several authors have reported the infrared and Raman spectra of PVDC [10-12].

Infrared absorption, Raman spectra, and inelastic neutron scattering from polymeric systems are very complex and cannot be unraveled without the full knowledge of their dispersion curves. Dispersion curves and dispersion profiles (line shape, if optically active) also provide information about the extent of coupling along the polymeric chain or between the chains. These curves also facilitate correlation of the microscopic behavior of a crystal with its macroscopic properties such as specific heat, enthalpy and free energy. The frequency of a given mode depends upon the sequence length of ordered conformation. Thus, the study of phonon dispersion in polymeric systems continues to be of topical importance.

In the present work, we report a complete normal mode analysis of PVDC using the Urey-Bradley force field,

including calculation of the phonon dispersion and heat capacity obtained via the density-of-states derived from the dispersion curves. The experimental data of IR and Raman spectroscopic studies reported by previous authors [12] have been used for comparison. Heat capacity has been calculated in the temperature range 50–500 K, which is in fairly good agreement with the experimental data [13]. Here it may be mentioned that various quantum chemical methods have been used for evaluation of vibrational frequencies. The advent of modern computers has enabled the handling of problems needing high speed. The most widely used theoretical quantum chemical method is the Density Functional Theory (DFT). The DFT method combines accuracy with computational speed. However, the vibrational frequencies obtained from these quantum chemical models do not always agree with the experimental measurements. Thus it has become a common practice to apply scaling factors. This scaling factor limits the accuracy as it, itself, varies over the frequency spectrum. The scaling factor also absorbs most of the anharmonic effects as well as errors due to it. The oligomer extrapolation generally used in DFT method for evaluating polymers dynamics, has its own limitations [14-17]. The Urey-Bradley force field, which considers non-bonded interactions as well as tension terms, does not suffer from this infirmity.

THEORETICAL APPROACH

NORMAL MODE CALCULATION

The calculation of normal mode frequencies was carried out according to the well-known Wilson's GF matrix method [18], as modified by Higgs [19]. The method consists of writing the inverse kinetic energy matrix G , and the potential energy matrix F , in terms of internal coordinates. In the case of an infinite

isolated helical polymer, there are an infinite number of internal coordinates that lead to G and F matrices of infinite order. The presence of screw symmetry in the polymer enables that a transformation similar to that given by Born and Von Karman can be performed that reduces the infinite problem to finite dimensions [20]. The vibrational secular equation gives normal mode frequencies and their dispersion as a function of phase angle and has the form:

$$|G(\delta)F(\delta) - \lambda(\delta)I| = 0, 0 \leq \delta \leq \pi \quad (1)$$

where δ is the phase difference between the vibrations of successive chemical repeat units of the polymer chain.

The vibrational frequencies $\nu(\delta)$ (in cm^{-1}) are related to the eigen values $\lambda(\delta)$ by the following relation:

$$\lambda(\delta) = 4\pi^2 c^2 \nu^2(\delta) \quad \dots\dots\dots (2)$$

CALCULATION OF SPECIFIC HEAT

Dispersion curves can be used to calculate the specific heat of a polymeric system. For a one-dimensional system, the density-of-state function, $g(\square)$, or the frequency distribution function, expresses the way the energy is distributed among various branches of normal modes in the crystal. It can be calculated from the relation:

$$g(\nu) = \sum_j (\partial \nu_j / \partial \delta)^{-1} \Big|_{\nu_j(\delta)=\nu} \quad (3)$$

with $\int g(\nu_j) \delta \nu_j = 1$

The sum is over all branches j , where j is the index for dispersion curves. Considering a solid as an assembly of harmonic oscillators, the frequency distribution $g(\square)$ is equivalent to a partition function. The constant volume heat capacity C_v can be calculated using

Debye's relation:

$$C_v = \sum_j g(\nu_j) k N_A (\hbar \nu_j / kT)^2 \frac{\exp(\hbar \nu_j / k)}{[\exp(\hbar \nu_j / kT) - 1]^2} \quad (4)$$

The constant volume heat capacity, C_v , given by the above equation is converted into constant pressure heat capacity, C_p , using the Nernst-Lindemann approximation [21, 22].

$$C_p - C_v = 3R A_o (C_p^2 T / C_v T_m^0) \quad (5)$$

Where A_o is a constant, often of a universal value [3.9×10^{-9} (Kmol/J)], and T_m^0 is the equilibrium melting temperature.

RESULT AND DISCUSSION

The number of atoms per residues [$\text{CH}_2\text{-CCl}_2$]_n in PVDC is six and hence there would be $(6 \times 3) - 4 = 14$ normal modes of vibration. The vibrational frequencies have been calculated for values of δ varying from 0 to π in steps of 0.05π . The assignments were made on the basis of potential energy distribution (PED), band intensity, band profile and absorption/scattering in similar molecules having groups placed in similar environments. The Urey-Bradley force constants were initially transferred from the earlier work on molecules having similar groups and were further refined by using the least-square deviation method [23]. Except for a couple of frequencies most of the frequencies are fitted within less than 1%. The optically active modes are those for which $\delta = 0, \pi, 2\pi$. The four zero frequencies correspond to acoustic modes, three representing translations along the three axes and one is rotation around the chain axis. All vibrational modes along with their potential energy distribution are given in Table 1 and Table

2 at $\delta = 0.0$ and $\delta = 1.0$, respectively.

DISPERSION CURVES

The dispersion curves below 1400 cm^{-1} are shown in Fig. 1(a). The modes above 1400 cm^{-1} were either non-dispersive or their dispersion was less than 5 cm^{-1} . A very interesting feature of the dispersion curves is the convergence of various modes. The modes that are separated by a large wave number at the zone center ($\delta = 0.0$) come very close at the zone boundary ($\delta = 1.0$). This convergence arises mainly because of phonon-phonon coupling and consequent sharing of potential energy in different measures by the coupled modes. The extent of sharing depends on the strength of coupling. For example, the two zone center modes calculated at 413 and 299 cm^{-1} are separated by 114 wave numbers but at the zone boundary they are separated by only 14 wave numbers. The P.E.D. of both modes at $\delta = 0.0$ and $\delta = 1.0$ are shown in Table 1 and Table 2, respectively. Similar features have been observed in the pair of modes, which appear at the zone center at 181 and 82 cm^{-1} .

Another specific feature of some of the dispersion curves was the exchange of character that occurs at repulsion points. For instance, the modes calculated at 757 and 703 cm^{-1} at the zone center showed repulsion at $\delta = 0.40$. These two modes have been separated by 55 wave numbers at $\delta = 0.0$, but at $\delta = 0.40$, they come close to each other, separated by only 15 wave numbers but again they repel to each other and separated by 107 wave numbers at $\delta = 1.0$. This phenomenon, in all probability, occurs due to intra-chain phonon-phonon coupling in the energy momentum space. It is like two phonons colliding in energy momentum space and separating after exchange of energy. This leads to the formation of regions of high

density-of-states (von Hove singularity).

HEAT CAPACITY

The dispersion curves obtained for PVDC have been used to calculate the density-of-states and heat capacity as a function of temperature. The density-of-states are shown in Fig. 1(b). Heat capacity of PVDC has been calculated in the temperature range $50\text{--}500\text{ K}$ (Fig. 2), which is in fairly good agreement with the experimental data [13].

It should be noted here that the contribution from the lattice modes is bound to make a difference to the heat capacity because of its sensitivity to low frequency modes. However, so far we have predicted the values only for an isolated chain. Calculation of dispersion curves for a three-dimensional system would be extremely difficult. Inter-chain modes involving hindered translatory and rotatory motion will appear and the total number of modes will depend on the contents of the unit cell. For each additional atom in the unit cell there is a 3-fold increase in the number of internal coordinates and it rapidly makes dimensionality of the problem prohibitive. The force field also simultaneously brings in an enormous number of interactions that are difficult to visualize and quantify. Thus the problem will become intractable. The inter-chain interactions will contribute primarily to lower frequencies. They are generally of the same order of magnitude as the weak intra-chain interactions. Their introduction will, at best, bring about crystal field splitting at the zone center and zone boundary depending on the symmetry-dependent selection rules. However, the intra-chain assignments will remain by and large undisturbed. Thus, in spite of several limitations involved in the calculation of specific heat, we believe the present work provides a good starting point for further

basic studies on the dynamic and thermodynamic behavior of polymers like PVDC. Complete 3-D studies have been reported only on polyethylene [24] and polyglycine [25, 26], where the unit cell is small. Other calculations with approximate interchain interactions, as in a β sheet of polypeptides, have been confined to

calculations of only zone center and zone boundary frequencies, by considering short segments and nearest neighbor interactions only [27]. The present work calculates the dispersion curves within the entire zone which is the only method to locate regions of high density-of-states which are important for thermodynamic behavior.

Table 1. Vibrational modes of PVDC at $\delta = 0.0$

Calculated	Observed		% PED (Potential Energy Distribution)
	IR	Raman	
2992	2987	3000	$\nu(\text{C-H})(99)$
2981	2982	2984	$\nu(\text{C-H})(99)$
1416	1409	1403	$\phi(\text{H-C-H})(41)+\phi(\text{H-C-C})(38)+\nu(\text{C-C})(17)$
1128	1142	1144	$\nu(\text{C-C})(73)+\phi(\text{H-C-H})(11)+\nu(\text{C-Cl})(5)$
1070	1070	1071	$\nu(\text{C-C})(76)+\nu(\text{C-Cl})(10)+\phi(\text{C-C-Cl})(5)$
974	980		$\phi(\text{H-C-C})(65)+\phi(\text{H-C-H})(14)+\tau(\text{C-C})(7)+\omega(\text{C-H})(7)$
757	752	748	$\phi(\text{H-C-C})(36)+\nu(\text{C-Cl})(35)+\nu(\text{C-C})(12)+\phi(\text{C-C-Cl})(10)$
703	688	688	$\phi(\text{H-C-C})(44)+\nu(\text{C-Cl})(30)+\tau(\text{C-C})(13)$
529	530	531	$\phi(\text{H-C-C})(40)+\nu(\text{C-Cl})(24)+\tau(\text{C-C})(17)+\phi(\text{C-C-C})(9)$
413	430		$\nu(\text{C-Cl})(27)+\tau(\text{C-C})(23)+\phi(\text{H-C-C})(23)+\phi(\text{C-C-C})(7)$
290	291	290	$\phi(\text{C-C-Cl})(66)+\phi(\text{C-C-C})(12)+\omega(\text{C-Cl})(8)+\nu(\text{C-Cl})(7)$
241	245	242	$\nu(\text{C-Cl})(37)+\phi(\text{C-C-C})(30)+\phi(\text{C-C-Cl})(24)$
225			$\phi(\text{C-C-Cl})(60)+\omega(\text{C-Cl})(10)+\nu(\text{C-Cl})(11)+\phi(\text{Cl-C-Cl})(7)$
181	185	184	$\phi(\text{Cl-C-Cl})(61)+\phi(\text{C-C-Cl})(31)$
82		99	$\phi(\text{C-C-Cl})(62)+\phi(\text{C-C-C})(13)+\tau(\text{C-C})(11)+\phi(\text{H-C-C})(6)$
34			$\tau(\text{C-C})(58)+\phi(\text{H-C-C})(29)$
6			$\phi(\text{C-C-C})(38)+\phi(\text{C-C-Cl})(32)+\tau(\text{C-C})(28)$

Table 2. Vibrational modes of PVDC at $\delta = 1.0$

Calculated	Observed		% PED (Potential Energy Distribution)
	IR	Raman	
2991	2987	3000	$\nu(\text{C-H})(99)$
2981	2982	2984	$\nu(\text{C-H})(99)$
1427	1409	1403	$\phi(\text{H-C-H})(40)+\phi(\text{H-C-C})(39)+\nu(\text{C-C})(15)$
1273	1265	1273	$\nu(\text{C-C})(71)+\phi(\text{H-C-H})(10)+\phi(\text{H-C-C})(7)+\nu(\text{C-Cl})(6)$
1012			$\phi(\text{H-C-C})(62)+\nu(\text{C-C})(17)+\tau(\text{C-C})(7)+\omega(\text{C-H})(5)$
899	886	879	$\nu(\text{C-C})(58)+\nu(\text{C-Cl})(21)+\phi(\text{C-C-C})(13)$
818			$\phi(\text{H-C-C})(59)+\tau(\text{C-C})(15)+\nu(\text{C-Cl})(9)+\phi(\text{H-C-H})(8)$
711			$\phi(\text{H-C-C})(25)+\tau(\text{C-C})(22)+\phi(\text{H-C-H})(20)+\nu(\text{C-Cl})(18)$
642	658	653	$\nu(\text{C-Cl})(44)+\phi(\text{H-C-C})(31)+\phi(\text{C-C-Cl})(10)+\nu(\text{C-C})(7)$
362	359	356	$\nu(\text{C-Cl})(87)+\nu(\text{C-C})(9)$
348	359	345	$\phi(\text{C-C-Cl})(55)+\phi(\text{C-C-C})(31)+\omega(\text{C-Cl})(8)$
264			$\phi(\text{C-C-Cl})(57)+\nu(\text{C-Cl})(18)+\phi(\text{C-C-C})(9)+\omega(\text{C-Cl})(9)$
188	185	184	$\phi(\text{Cl-C-Cl})(68)+\phi(\text{C-C-Cl})(26)+\omega(\text{C-Cl})(5)$
103	102	99	$\phi(\text{C-C-C})(44)+\phi(\text{C-C-Cl})(36)+\nu(\text{C-C})(6)$
89		99	$\phi(\text{C-C-Cl})(74)+\omega(\text{C-Cl})(9)+\tau(\text{C-C})(7)$
34			$\tau(\text{C-C})(45)+\phi(\text{H-C-C})(29)+\phi(\text{C-C-C})(19)$
5			$\phi(\text{C-C-C})(45)+\tau(\text{C-C})(28)+\phi(\text{H-C-C})(19)+\phi(\text{C-C-Cl})(5)$

Note: All frequencies are in cm^{-1} .

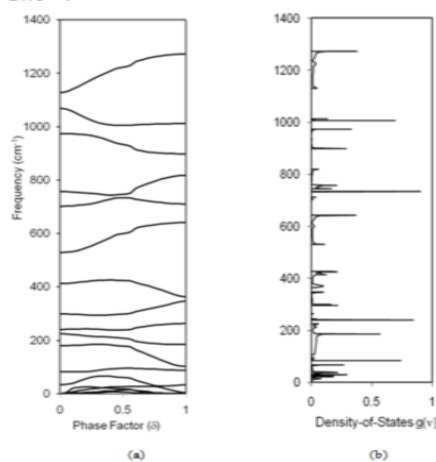


Fig. 1. (a): Dispersion curves of PVDC (0-1400 cm^{-1}) (b): Density-of-states of PVDC (0-1400 cm^{-1}).

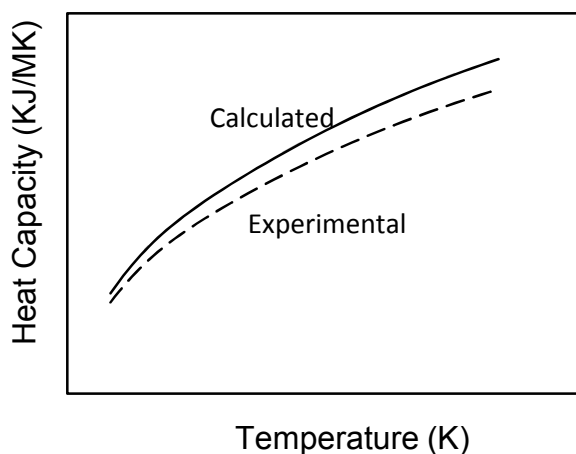


Fig. 2. Variation of heat capacity with temperature of PVDC.

CONCLUSION

The vibrational dynamics of PVDC have been satisfactorily interpreted from the dispersion curves and dispersion profiles of the normal modes of PVDC as obtained by Higg's method for infinite systems. Some of the internal symmetry-dependent features, such as attraction and exchange of characters are also well understood. Heat capacity behavior of PVDC with temperature was observed nearly linear in nature. Heat capacity provides a relationship between microscopic behavior and a macroscopic property. In addition, the thermal stability of a polymeric system and its interactive nature with other properties, such as phonon-phonon coupling is also related to thermodynamic behavior. It also provides a theoretical framework to understand experimental measurements.

REFERENCES

- [1]. Li Yuesheng, W. Zhixue, H. Zhiming and P. Zuren, *Chin. J. Polym. Sci.* 14 (1996) 105.
- [2]. K.K. Mokwena, J. Tang, *Crit. Rev. Food Sci. Nutr.* 52 (7) (2012) 640.
- [3]. G.L. Robertson, *Food Packaging: Principles and Practice*, Third ed. Chapter 2, 2013.
- [4]. L.K. Massey, *Permeability Properties of Plastics and Elastomers*, Second ed. Chapter 59, 2003.
- [5]. B.A. Howell, B.S. Warner, C.V. Rajaram, S.I. Ahemed and Z. Ahmed, *Polym. Adv. Technol.* 5 (1994) 485.
- [6]. A. Konishi, *Bull. Chem. Soc. Jpn.* 35 (2) (1962) 193.
- [7]. A. Konishi, *Bull. Chem. Soc. Jpn.* 35 (2) (1962) 197.
- [8]. K. Matsuo, G.W. Nelb, R.G. Nelb and W.H. Stockmayer, *Macromole.* 10 (1977) 654.
- [9]. J.D. Burnett and H.W. Melville, *Trans. Faraday Soc.* 46 (1950) 976.
- [10]. S. Narita, S. Ichinohe and S. Enomoto, *J. Polym. Sci.* 37 (131) (1959) 251-261.
- [11]. S. Krimm and C.Y. Liang, *J. Polym. Sci.* 22 (1956) 95-112.
- [12]. M.S. Wu, P.C. Painter and M.M. Coleman, *J. Polym. Sci: Polym. Phys. Ed.* 18 (1980) 95.
- [13]. U. Gaur, B.B. Wunderlich and B.

- Wunderlich, J. Phys. Chem. Ref. Data 12 (1983) 31.
- [14]. C.X. Cui and M. Kertesz, J. Chem. Phys. 93 (1990) 5257.
- [15]. C.X. Cui, M. Kertesz and Y. Jiang, J. Phys. Chem. 94 (1990) 5172.
- [16]. C.X. Cui and M. Kertesz, Macromole. 25 (1992) 1103.
- [17]. C.X. Cui, M. Kertesz and H. Eckhardt, Syn. Met. 43 (1991) 3491.
- [18]. E.B. Wilson, J.C. Decuis and P.C. Cross, Molecular Vibrations: The theory of
- [19]. Infrared and Raman vibrational spectra, Dover Publications, New York, 1980.
- [20]. P.W. Higgs, Proc. Roy. Soc. A 220 (1953) 472.
- [21]. P. Tondon, V.D. Gupta, O. Prasad, S. Rastogi and V.P. Gupta, J. Polym. Sci. Part B: Polym. Phy. 35 (1997) 2281.
- [22]. R. Pan, M.N. Verma and B. Wunderlich, J. Therm. Anal. 35 (1989) 955.
- [23]. K.A. Roles, A. Xenopoulos and B. Wunderlich, Biopolymers 33 (1993) 753.
- [24]. P. Ali, S. Srivastava, S.I. Ansari and V.D. Gupta, Spectrochim. Acta A Mol. Biomol. Spectrosc. 111 (2013) 86.
- [25]. S. Krimm, C.Y. Liang and G.B.B.M. Sutherland, J. Chem. Phys. 25 (1956) 549.
- [26]. Y. Abe and S. Krimm, Biopolymers 11 (1972) 1817.
- [27]. V.D. Gupta, S. Trevino and H. Boutin, J. Chem. Phys. 48 (1968) 3008.
- [28]. S. Krimm, Vibrational Spectroscopy of Polypeptides in Modern Polymer Spectroscopy ed. G. Zerbi, Wiley-VCH, Weinheim, Chapter 5, 1999.